Journal of Molecular Liquids 261 (2018) 146–154

Contents lists available at ScienceDirect

Journal of Molecular Liquids

journal homepage: www.elsevier.com/locate/molliq

Modification of activated carbon with magnetic Fe_3O_4 nanoparticle composite for removal of ceftriaxone from aquatic solutions

Mojtaba Yegane Badi [a,b], Ali Azari [c], Hasan Pasalari [b], Ali Esrafili [a,b], Mahdi Farzadkia [a,b,*]

[a] Research Center for Environmental Health Technology, Iran University of Medical Sciences, Iran
[b] Department of Environmental Health Engineering, School of Public Health, Iran University of Medical Sciences, Tehran, Iran
[c] Department of Environmental Health Engineering, School of Public Health, Kashan University of Medical Sciences, Kashan, Iran

ARTICLE INFO

Article history:
Received 1 January 2018
Received in revised form 3 April 2018
Accepted 4 April 2018
Available online 7 April 2018

Keywords:
Adsorption
Powdered activated carbon (PAC)
Fe_3O_4
Ceftriaxine
Response Surface Methodology (RSM)

ABSTRACT

Recently, Antibiotics have been extensively applied in various industries including agricultural, pharmaceutical and veterinary. Great concerns of antibiotics are about discharge into environment, especially water sources supplied for water demand over the world. The present study was developed to investigate the performance of powder activated carbon modified with magnetite nanoparticles (PAC-MNPs) in removal of Ceftriaxone from aquatic solutions with response surface methodology (RSM). A co-precipitation was applied to synthesize magnetized powdered activated carbon and its characteristics were analyzed with TEM, SEM and XRD. The effects of independent parameters pH (3−11), initial Ceftriaxone values (10–100 mg/L), temperature (298–313 K), and adsorbent dosage (1.05–2 g/L) on removal efficiency were analyzed by RSM based Box-Benhken Design (BBD). The optimum conditions for maximum removal of Ceftriaxone (97.18% with desirability of 0.9720) were recorded from desirability function (DF) at pH: 3.14, contact time: 90 min, adsorbent dosage: 1.99 g/L, initial concentration: 10 mg/L and temperature: 298 K. The survey of isotherms and Kinetics indicated that the experimental data are fitted to Langmuir and second-pseudo-order models. Thermodynamic studies revealed that the CTX removal was spontaneous and exothermic. Regeneration experiments were performed for 6 cycles and the results indicate a removal efficiency loss of <10%.

1. Introduction

Recently, the studies on treatment of emerging contaminants (EC) including, antibiotic, insecticide, pharmaceutical, and personal care product (PCP) have been attracted considerably because conventional treatment systems are not capable of eliminating these pollutants [1–3]. These contaminants accumulate in surface and groundwater water sources, and accordingly cause health risks for both human and environment [4]. Furthermore, Over-consuming of antibiotics over the past few decades has forced researchers to find new techniques in order to deal with or better management of this issue [5]. Ceftriaxone (CTX), as an antibiotic, is extensively applied to treat respiratory tract infection (RTI), urinary system infection and gonorrhea. It poses potential risks to aquatic ecosystem and human health due to recalcitrant molecular structure, as its chemical structure is shown in Table 1 [6]. In the last few decades, various techniques i.e. chemical oxidation [7], Ion exchange [8], Biological treatment [9], photochemical degradation [10], and adsorption [11] have been utilized for CTX removing from aqueous solutions, but each one has its own disadvantages. The most important problems with these techniques are high energy consuming, high initial investment, low mineralization efficiency of antibiotics. Due to simplification, high removal efficiency, no harmful by-products, and potential of reusing, adsorption on the activated carbon has been considered as a suitable method for CTX removal from aqueous solution [11,12]. The main drawback of the powdered absorbents such as PAC in water and wastewater treatment systems is difficulty to separation from the effluents samples. In most previous studies, the adsorbent separation is carried out by filtration and centrifugation methods. The mentioned methods have mainly developed additional costs. On the other hand, these techniques may not be able to completely isolate the absorbent from the sample, and instead result in the formation of secondary turbidity. To overcome the problems described, a magnetized activated carbon is suggested as appropriate solution. In this method, modification of activated carbon with iron oxide (Fe_3O_4 MNPs) as a magnetic source, used for quick and easy separation of adsorbent and adsorbed contaminate by an external magnetic field [13,14]. Azari et al. reported that the presence of Fe_3O_4 MNPs leads to chemical stability and excellent recyclability of adsorbent for removal of toxic ions and organic contaminants from water and wastewater [15]. The regeneration ability of the magnetic adsorbents represent that these green technologies can be applied at full-scale wastewater treatment (industrial application) for many times, as well as batch-adsorption tests. The irrefutable advantages of the PAC-MNPs adsorbent including inexpensive preparation

* Corresponding author.
E-mail address: farzadkia.m@iums.ac.ir. (M. Farzadkia).

https://doi.org/10.1016/j.molliq.2018.04.019
0167-7322/

Table 1
Chemical specifications of Ceftriaxone.

Molecular	Ceftriaxone Sodium
Chemical formula	$C_{18}H_{18}N_8O_7S_3$
Chemical structure	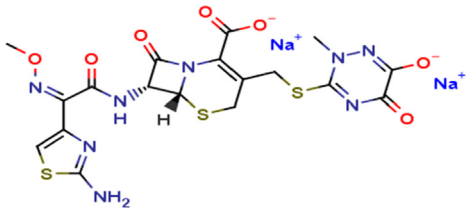
Molecular weight	661.60
Density	0.35 g/mL

method, good adsorption capacity and high separation rate via an external magnetic field, recommend it as a promising candidate for the removal of CTX from aqueous solutions [16].

So far, a few studies have been investigated the remediation of antibiotic- contaminated water by sorption on magnetic activated carbon. For example, Danalıoğlu et al. recently reported that the magnetic activated carbon/chitosan (MACC) is a promising technique for antibiotic removal from aquatic solutions [17]. In another research, the feasibility of activated carbon was investigated in removal of 28 different antibiotics [18]. In 2014, Kakavandi [19] conducted a study on Amoxcocilin removal and found that the Fe_3O_4@C nanoparticles had the proper ability to remove this organic matter from aquatic solutions. However, despite the above-mentioned studies, no report on the removal of CTX by PAC-MNPs are not provided. Almost all research about adsorption process have been carried out in batch systems without considering the number of

required experiments, expense, time-saving and decrease in the consumption of reagent and material as well. To overcome the each of the above problems and achieve the best probable response, the optimization process is the key solution. Box-Behenken design (BBD) is established to be the most extensively used optimization method for the adsorption process because of the benefits of optimizing several factor problems with the best number of test runs according to response surface methodology (RSM) [20].

Given the issues that were addressed, the objectives of this study were (i) synthesized of powdered activated carbon magnetized with Fe3O4 nanoparticles and it's extensively characterized using TEM, SEM, and XRD; (ii) investigating the effect of key variables such as pH, contact time, temperature, CTX initial concentration and PAC-MNPs dosage on the adsorptive removal of CTX from aqueous solution using experimental design approach based on the Box-Behenken design (BBD) (iii) Investigating the adsorption equilibrium, kinetic and thermodynamic to examine adsorption behavior of CTX onto the PAC-MNPs and (IV) Investigating the stability and reusability of the adsorbent under six consecutive cycles.

2. Methods and material

2.1. Chemicals and instruments

In the present study, all used chemicals and reagents including Hexa Chloride Ferric ($FeCl_3.6H_2O$), Tetrachloride Ferric ($FeCl_2.4H_2O$), CTX, Nitric Acid (HNO_3), Ammonium, and powdered activated carbon were in analytical grade and purchased from Merck Company (Germany). Deionized water was used throughout the experiments. To specify the residual CTX in the experiments, the High-performance liquid chromatography (HPLC) (Cecil 4100 Powerstream Interface, England) was used. The pH was measured using Metrohm pH meter (Swiss, model-827). For keeping a constant temperature and mixing solutions, a shaker incubator (n-BioTEK NB-205) was utilized. A magnet with the magnetic strength field of 1.3 Tesla used for separation of PAC-MNPs.

2.2. Magnetizing of activated carbon with Fe_3O_4

A co-precipitation method was employed to synthesize magnetized activated carbon powder [21]. To promote the porosity and specific area of activated carbon, 100 cm^3 HNO_3 with purity of 63.1% was added to 10 g of PAC and then placed on shaker (200 rpm) for 30 min; then, passed through the Wattman filter with 0.45 μm in size. The PAC was rinsed with deionized water several times until the pH of drained water reached 7 ± 0.2, and then dried in oven at 80 °C for 24 h. After that, in order to Fe_3O_4 nanoparticle bonding to the PAC, 8 g $FeCl_3$ and 2.5 g $FeCl_2$ were mixed to the dried activated carbon. This stage was performed in an ultrasonic bath under N_2 gas. Then, to create co-precipitation process of Fe_3O_4 nanoparticles on the surface of PAC, a 50 cm^3 of ammonia (25% purity) were gradually added to the mixture [22,23]. The co-precipitation method with Fe^{2+} and Fe^{3+} ions which react in alkaline conditions to magnetite formation [24–28], following as:

$$Fe^{3+} + 3OH^- = Fe(OH)_3\ (s) \quad (1)$$

$$Fe(OH)_3\ (s) = FeOOH\ (s) + H_2O \quad (2)$$

$$Fe^{2+} + 2OH^- = Fe(OH)_2\ (s) \quad (3)$$

$$2FeOOH\ (s) + Fe(OH)_2\ (s) = Fe_3O_4\ (s) + 2H_2O \quad (4)$$

Giving an overall reaction:

$$2Fe^{3+} + Fe^{2+} + 8OH^- = 2Fe(OH)_3Fe(OH)_2\ (s) \rightarrow Fe_3O_4\ (s) + 2H_2O \quad (5)$$

Initially, the ferric and ferrous hydroxides are precipitated. These reactions occur at very fast rate. Secondly, as the low water activity of the resulting NaCl solution in a slower reaction, the ferric hydroxide degrades to FeOOH. Finally, a solid state reaction between FeOOH and Fe $(OH)_2$ takes place, due to the low water activity of the solution, which produces magnetite. This solid state reaction takes place between 10 and 30 min at room temperature. The overall reaction mechanism is a dynamic equilibrium equation in which the concentration and size of Fe_3O_4 nanoparticles are affected by $[Fe^{3+}]$, $[Fe^{2+}]$ and $[OH^-]$, as well as the water activity of the solution.

2.3. Characterization of prepared PAC-MNPs

In the current study, transmission electron microscope (TEM, PHILIPS, EM) at 100 kV was used to characterize the shape and size of synthesized PAC-MNPs. A scanning electron microscopy (SEM) (CamScan, MV 2300) was applied to determine surface and morphology of PAC and PAC-MNPs as well as the size of magnetized nanoparticles. The crystallographic pattern of PAC was determined by X-ray diffraction (XRD) method on an X-ray diffractometer (PANalytical X'Pert PRO XRD, Germany) with Cu-kα radiation (λ = 1.54 Å at 25 °C, 45 kV, 40 mA). The

Table 2
Isotherm equations and their Linear and non-linear relationships.

Model	Non-linear form	Linear form	Equation number
Langmuir	$q_e = \frac{q_{max} K_L\ C_e}{1+K_L\ C_e}$	$\frac{C_e}{q_e} = \frac{C_e}{q_{max}} + \frac{1}{K_L q_{max}}$	(8)
Freundlich	$q_e = K_F\ C_e^{1/n}$	$\ln q_e = \ \ln K_f + \frac{1}{n} + \ \ln C_e$	(9)
Temkin	$q_e = \frac{RT}{b_t}\ \ln(a_t\ C_e)$	$q_e = A + B \ln\ C_e$	(10)

experiments related to pHzpc of the adsorbent were performed at pH range 2–12. At first, 100 mL of PAC-MPNs solution was transferred to a series of Elnermayer fasks and then pH was adjusted to desirable values by adding a few drops of 0.1 M HCl or 0.1 M NaOH solutions. After that, 0.2 g of PAC-MPNs was added to each flask and the final pH was measured after 48 h under agitation at room temperature. The difference between the initial (pHi) and the final pH (pHf) values ($\Delta pH = pHi - pH_f$) was plotted against the initial pH (pHi). The pHzpc is the point of intersection of the resulting curve at which pH = 0.

2.4. Analysis and measurement methods

To specify and determination of CTX in the experiments, the high performance liquid chromatography (HPLC, Cecil 4100 Power stream Interface, England) equipped with the UV–visible detector (4900 CE) at 240 nm was used. 20 μL of samples were injected in a C18 column (250 mm × 4.6 mm), using a mixture of acetonitrile and 0.05 M Na_2HPO_4 at pH = 7.6 as mobile phase. The mobile phase was pumped at flow rate of 1.0 mL/min.

2.5. Experiments methodology

In current study, the effect of different variables such as initial concentration of CTX, adsorbent dosage, pH, temperature, and contact time on the removal of CTX were investigated. For this purpose, a 1000 mg/L of CTX stock solution was prepared with deionized water and then diluted in different concentrations. The pH of solution was adjusted by addition of 0.1 N NaOH and HCl solutions. All experiments were examined in an Erlenmeyer flask. The solutions were placed on shaker incubation (120 rpm) and when the target contact time was reached, the adsorbent was separated from solution by an external magnet; afterwards, a 20 μL of sample solution was injected to HPLC to specify the residual CTX. The amount of CTX adsorbed (q_e, mg/g) onto the adsorbent was calculated using the following equation:

$$qe = (C_0 - C_e) * \frac{V}{M} \tag{6}$$

where C_0 (mg/L) is the initial concentration of CTX, C_e (mg/L) is equilibrium concentration of CTX, M (mg) is mass of adsorbent and V (L) is volume of solution.

2.6. Adsorption isotherms

The study on equilibrium adsorption isotherms of CTX was conducted at optimum conditions. The Langmuir, Freundlich and Temkin models were used to investigate the adsorption isotherms of CTX at 10, 25, 50, 75 and 100 mg/L concentrations. Each isotherm model was expressed by relative certain constants which characterized the surface properties and indicated adsorption capacity of this material. Langmuir isotherm model is defined as a one-layer and homogenous adsorption of adsorbate with equal energy on entire the adsorbent surface [29]. The Freundlich isotherm is an empirical equation that assumes that the adsorption process occurs on heterogeneous surfaces with non-uniform distribution of adsorption heat. The Temkin isotherm model proposed the impact of some indirect adsorbent–adsorbate interactions on adsorption isotherms [19]. The linear and non-linear equations of mentioned isotherm models are shown in Table 2 [30].

In Table 2, Ce (mg/L) is the equilibrium concentration, q_e (mg/g) is the rate of the adsorbed CTX per mass unit of the absorbent, K_L (L/mg) represents Langmuir constant, q_{max} (mg/g) is the maximum adsorption capacity of adsorbent. The parameters qe and k_l were calculated from the slope and intercept of the plot of $\frac{C_e}{q_e}$ against Ce. n and K_f (1 mg/g(L/mg)^n) are Freundlich constant and the intensity of adsorption, respectively. R (8.314 J/mol K) is the universal gas constant and T (°K) is the absolute temperature, and A ($(RT/b_t)\ ln a_t$) and B (RT/b_t) are considered as constants of the Temkin isotherm. One of the important parameters that is discussed in Langmuir isotherm is RL. The RL parameter is the dimensionless constant factor which indicates the affinity of adsorbed material to the adsorbent and calculated using Eq. (7):

$$R_L = \frac{1}{1 + K_L C_e} \tag{7}$$

Based on R_L factor the nature of the isotherm to be classified as follows: $\mathbf{R_L > 1}$: unfavorable isotherm;

$\mathbf{R_L = 1}$: linear isotherm; $\mathbf{0 < R_L < 1}$: favorable isotherm and $\mathbf{R_L < 1}$: irreversible isotherm.

2.7. Adsorption kinetics

Adsorption kinetic provides imperative information about the adsorption mechanism and velocity of adsorption process. For the kinetic study of CTX adsorption on PAC-MNPs, the influencing parameters were considered in optimum condition at 0 to 90 min. In the present work, three kinetic equations i.e. Pseudo-first-order, Pseudo-second-order and Intra-particle diffusion were applied to analyze the kinetic adsorption of CTX on PAC-MNPs; the linear and non-linear forms of these equations are presented in Table 3 [31,32].

In Table 3, q_t (mg/g) is the adsorbed CTX per mass unit of the absorbent at the time of t, K_1 (1/min) is Pseudo-first-order rate constant, qe (mg/g) is the adsorbed CTX per mass unit of the absorbent at the equilibrium time. K_2 (1/min) is Pseudo-second-order rate constant, t (min) is the contact time. K_0 is the intercept and K_{id} (mg/g/min$^{-1/2}$) is the intraparticle diffusion rate constant.

Table 3
Kinetic models and their linear and non-linear forms.

Model	Non-linear form	Linear form	Equation number
Pseudo-first order	$q = q_e\ (1 - exp^{-K_1 t})$	$\ln(q_e - q_t) = \ln\ (q_e) - k_1 t$	(11)
Pseudo-second order	$q = \frac{K_2 q_e t}{1+K_2 q_e t}$	$\frac{t}{q_t} = \frac{1}{k_2 q_e^2} + \frac{t}{q_e}$	(12)
Intra-particle diffusion	$q_t = K_{id} t^{1/2} + K_0$	$q_t = K_{id} t^{1/2} + K_0$	(13)

Table 4
Independent variables and their ranges.

Parameters	Abbreviation	-1	0	+1
pH	X_1	3	7	11
Contact time (min)	X_2	5	47.5	90
Concentration (mg/L)	X_3	10	55	100
Adsorbent dosage(g/L)	X_4	0.1	1.05	2
Temperature (K)	X_5	298	305.5	313

2.8. CTX thermodynamic studies

In order to investigation the effect of temperature on the adsorption efficiency of CTX onto the prepared sorbent, the thermodynamic study was applied in three different temperature values (298.15, 305.65 and 313.15 K). It is important to note that the other affecting parameters were considered in optimum conditions.

The adsorption standard free energy changes (ΔG°) can be calculated according to

$$\Delta G = -RT(\ln K_C) \quad (14)$$

where ΔG° (kJ/mol) indicates the Gibbs standard free energy change, T (°K) is the temperature, R (8.314 J mol K) is the universal gas constant, K_c (L/g) is a constant that is calculated from Eq. (15).

$$K_c = \frac{q_e}{C_e} \quad (15)$$

qe (mg/g) and Ce (mg/L) are the equilibrium concentration of CTX on the PAC-MNPs and in the solution respectively. The average standard enthalpy change (ΔH°) is obtained from Van't Hoof equation,

$$\ln k_c = \frac{\Delta S^0}{R} - \frac{\Delta H^0}{RT} \quad (16)$$

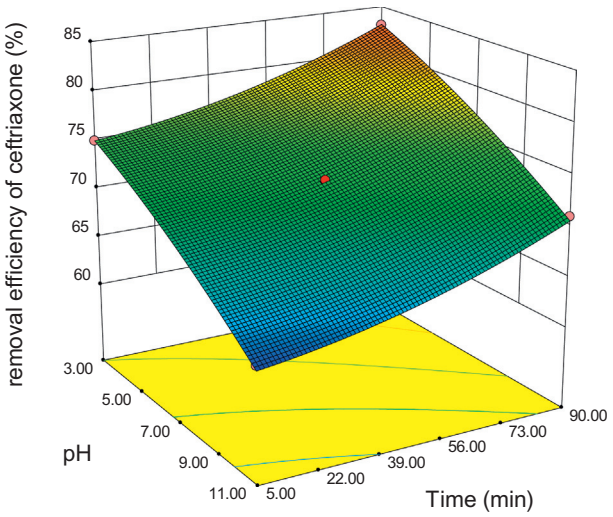

Fig. 2. The effect of pH on the removal percentage of CTX (Adsorbent dose = 1.05 g/L, Temperature = 305.5 K, Concentration CTX = 55.0 mg/L).

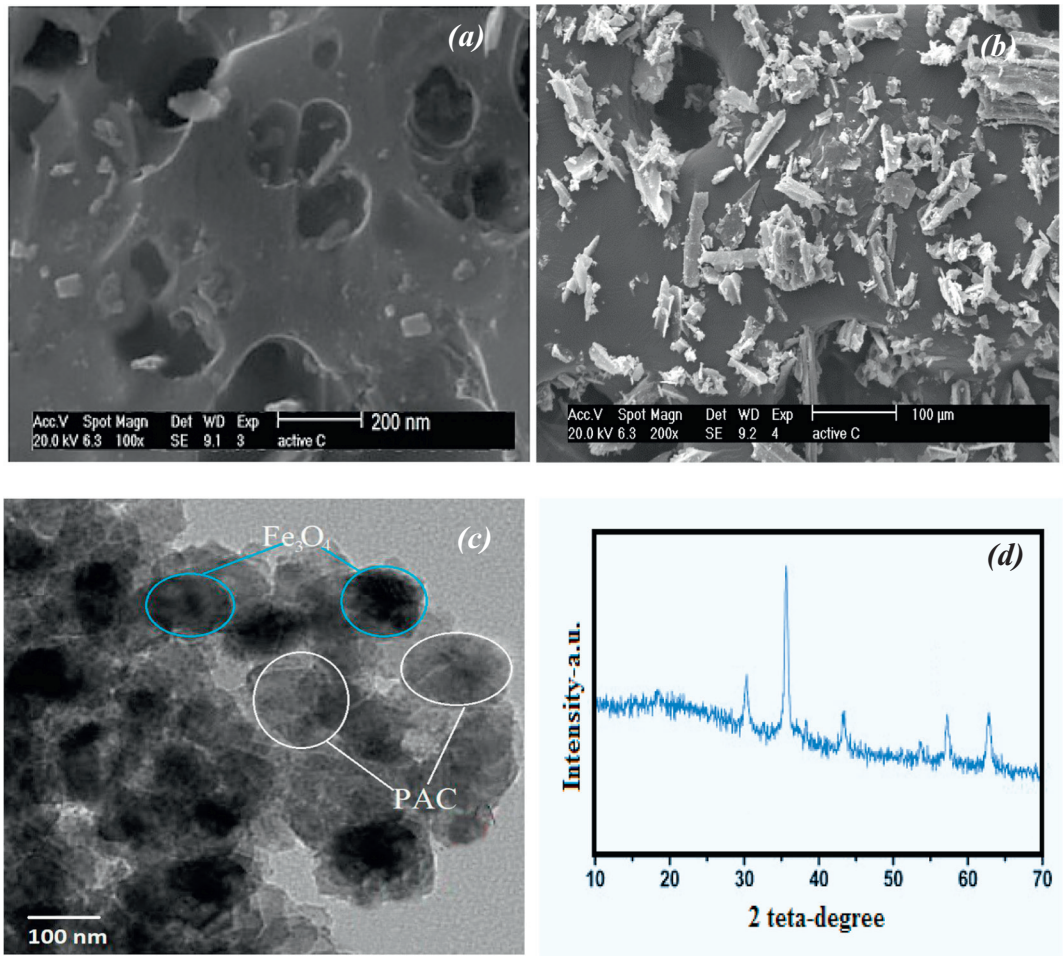

Fig. 1. SEM images of PAC (a) and PAC-MNPs (b), TEM (c) and XRD (d) of PAC-MNPs.

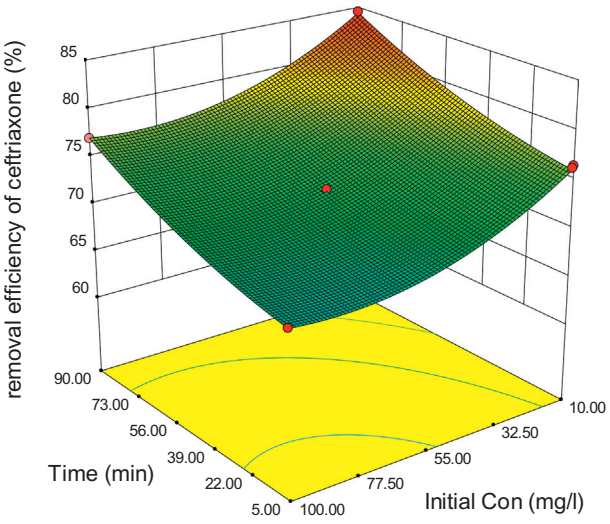

Fig. 3. The effect of concentration on the removal percentage of CTX (Adsorbent dose = 1.05 g/L, Temperature = 305.5 K, pH = 7.0).

The standard entropy change (ΔS°) can be obtained by

$$\Delta G = \Delta H^0 - T\,\Delta S^0 \tag{17}$$

2.9. Adsorption optimization

Using the Response Surface Methodology (RSM) and basis on Box-Behnken design (Design Expert 10.0), the effect of five parameters including pH, contact time, initial concentration of CTX and dosage of PAC-MNPs on removal efficiency were investigated and listed in Table 4. The Eq. (18) was employed to determine the CTX removal [16,33].

$$E = \frac{C_0 - C_e}{C_0} * 100 \tag{18}$$

where C_0 (mg/L) is the initial concentration of CTX, C_e (mg/L) is equilibrium concentration of CTX, E indicates the removal efficiency of CTX (%).

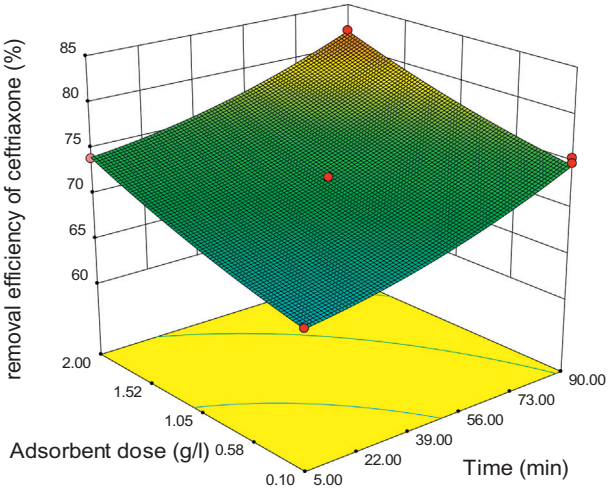

Fig. 4. The effect of PAC concentration on the removal percentage of CTX (Concentration CTX = 55.0 mg/L, Temperature = 305.5 K, pH = 7.0).

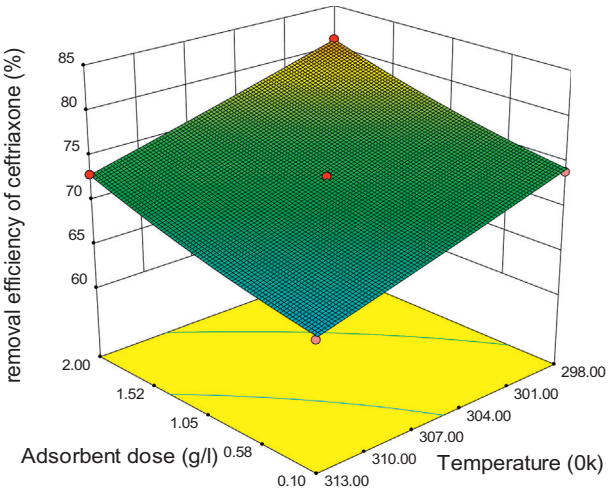

Fig. 5. The effect of temperature on the removal percentage of CTX (Concentration CTX = 55.0 mg/L, Time = 47.5 min, pH = 7.0).

The behavior of the adsorption process can be explained based on the following empirical second order polynomial model Eq. (19):

$$Y = b_0 + \sum_{i=1}^{n} b_i X_i + \sum_{i=1}^{n} b_{ii} X_i^2 + \sum_{i=1}^{n-1} \sum_{j=i+1}^{n} b_{ij} X_i X_j \tag{19}$$

where, Y is the predicted response (CTX removal efficiency), b_0 is a constant while, bi, b_{ii} and b_{ij} stand for the linear coefficient, quadratic coefficient and interaction effect coefficient, respectively. X_i and X_j are also the coded values of the variables. In addition, analysis of variance (ANOVA) was used to analyze the results and also to check the statistical significance of the fitted quadratic models. The optimal values of the critical parameters for adsorption process were calculated by using the fitted models and then validated based on the results of the experiments.

Table 5
Results of ANOVA analysis in the Square Surface Response Model to determine the efficiency of CTX adsorption.

Source	Sum of squares	df	Mean square	F Value	p-Value prob. > F	
Model	1593.55	20	79.68	1976.03	<0.0001	significant
X_1-pH	576.00	1	576.00	14,285.02	<0.0001	
X_2-Time	260.02	1	260.02	6448.49	<0.0001	
X_3-Concentration	216.09	1	216.09	5359.11	<0.0001	
X_4-Adsorbent dose	191.13	1	191.13	4740.11	<0.0001	
X_5-Temperature	256.00	1	256.00	6348.90	<0.0001	
$X_1 X_2$	0.000	1	0.000	0.000	1.0000	
$X_1 X_3$	0.063	1	0.063	1.55	0.2262	
$X_1 X_4$	0.063	1	0.063	1.55	0.2262	
$X_1 X_5$	0.000	1	0.000	0.000	1.0000	
$X_2 X_3$	0.000	1	0.000	0.000	1.0000	
$X_2 X_4$	0.063	1	0.063	1.55	0.2262	
$X_2 X_5$	0.000	1	0.000	0.000	1.0000	
$X_3 X_4$	0.12	1	0.12	3.04	0.0953	
$X_3 X_5$	0.000	1	0.000	0.000	1.0000	
$X_4 X_5$	0.000	1	0.000	0.000	1.0000	
X_1^2	5.14	1	5.14	127.38	<0.0001	
X_2^2	8.40	1	8.40	208.39	<0.0001	
X_3^2	48.55	1	48.55	1203.98	<0.0001	
X_4^2	2.53	1	2.53	62.83	<0.0001	
X_5^2	0.069	1	0.069	1.72	0.2029	
Residual	0.89	22	0.40			
Lack of Fit	0.65	20	0.032	0.27	0.9573	not significant
Pure Error	0.24	2	0.12			
Cor Total	159.444	42				

R^2 = 0.9573, adjusted-R^2 = 0.9989, R^2-Predicted = 0.9980, Adeq precision = 159.610.

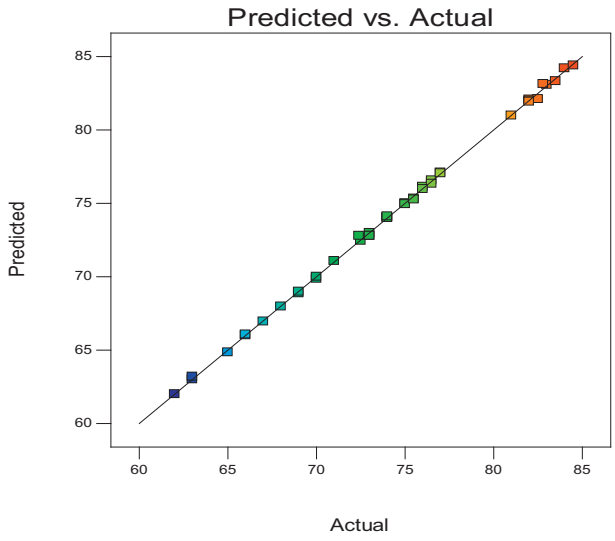

Fig. 6. Comparison between the experimental values and the predicted values of RSM model.

2.10. Reusability of PAC-MPNs

The regeneration of adsorbent is key criteria for the recovery of pollutants from wastewater. Therefore, a number of tests were performed under the optimum conditions obtained earlier. For this reason, the studied adsorbent (2 g/L) underwent six consecutive adsorption-desorption cycles at a given concentration of the analyte (10 mg/L) were considered. It is worth noting that at the end of each adsorption cycle, desorption experiments were carried out using methanol solution as a desorbing agent. The adsorbent was thereafter repeatedly washed with DI-water and finally dried in an oven and reused for the subsequent adsorption-desorption cycle.

3. Results and discussion

3.1. Characterization of PAC-MNPs

The surface morphology of activated carbon before and after modification was determined by scanning electron microscopy (SEM). The surface morphology of PAC and PAC-MNPs are shown in Fig. 1(a and b). SEM analysis shows that the external adsorbent surface is rough and has some cavities. It also indicates that cavities have been relatively distributed uniformly on the adsorbent surface with various sizes and shapes. The TEM analysis of the adsorbent (Fig. 1(c)) reveals that Fe3O4 particles with a polygonal structure and diameter <75–100 nm distributed on PAC. These results also confirmed the successful synthesis of Fe3O4 nano-crystals on the PAC surface. The XRD patterns of the synthesized adsorbent in the 2θ range of 10–70° show a narrow diffraction peak at 2θ = 35.5°. The peak points created with diffraction angle at 35° in XRD diffractograms confirm that the Fe_3O_4 nanoparticles were attached to the prepared powdered activated carbon successfully.

3.2. The effect of pH on CTX adsorption

The effect of pH and contact time variation on the adsorption efficiency of CTX on the PAC-MNPs are presented in Fig. 2. As can be seen, by increasing the contact time from 0 to 90 min and decreasing pH from 11 to 3, the removal efficiency of CTX was increased. The pH of solution is one critical factor in contaminant removal and adsorption process. The results obtained from the present research show that the highest removal efficiency value occurs at pH 3, and the removal efficiency was decreased as the pH value was increased [34,35]. The number of protons rise up as pH value is decreased to acidic range, these protons were adsorbed onto the adsorbent, and as a result, induce positive electrical charge on the adsorbent. A decline in removal efficiency in alkanity conditions is assumed to be results from reduction in electrostatic affinity between PAC-MNPs with negative-ion surface and anions in active sites onto adsorbent [35,36]. On the other hand, CTX has negative electrical charge; the positive electrical charge on the adsorbent and negative charge of the CTX create an electrostatic gravity force and finally, it leads to greater CTX adsorption on the PAC-MNPs [37,38]. In a study that conducted by Liu et al. the optimum pH for Norofleuxacine removal was reported at acidic pH which it is in line with the present work [39]. Besides, in another study, Kakavandi et al. concluded that the optimum pH for Amoxicillin removal using magnetized powdered activated carbon with Fe_3O_4 is in acidic range [40]. The point of zero charge (pzc) for PAC-MNPs is 6.4 thus, the surface of PAC-MNPs will be positively charged at pH < 6.4, and negatively charged at pH > 6.4, and neutral for pH = 6.4. Also, CTX has electron rich aromatic rings tending to be adsorbed on the positively charged surface of adsorbent. Considering the pK_a values of Ceftriaxone (pK_{a1} = 1.72, pK_{a2} = 3.15 and pK_{a3} = 4.34) [41], it is assumed that ionic species of Ceftriaxone varies from neutral charge at acidic pH values to negative charge at neutral and alkaline pH, which confirms the acceleration in the adsorption efficiency of Ceftriaxone.

3.3. The effect of initial concentration on CTX adsorption

The effect of various initial concentration of CTX (ranged between 10 and 100 mg/L) on adsorption efficiency was surveyed and the obtained results are shown in Fig. 3. As the Fig. 3 shows, the results of present study indicate that increases in initial concentrations of CTX solutions from 10 to 100 mg/L give rise to reduction of removal efficiency. The highest removal efficiency was obtained at initial concentration equal to 10 mg/L. As active adsorption sites on the surface of a adsorbent is constant, when the concentration of adsorbate increases in solution, the available active adsorbent site would be reduced and as a result, the adsorption of adsorbate would be decreased [42,43].

3.4. The effect of PAC-MNPs dosage on CTX adsorption

The effect of different adsorbent dosage (0.1–2 g/L) on CTX removal efficiency were investigated. As shown on Fig. 4, the removal efficiency of CTX enhances by increasing adsorbent dosage and the highest efficiency was found to be in dosage levels of 2 g/L. Considering the obtained results, it can be concluded that the highest CTX removal occurred in adsorbent dosage equal to 2 g/L. Adsorbent dosage is an effective parameter in removal efficiency, because the greater amount of adsorbent prepares more free sites onto adsorbent in order to adsorb the adsorbate. Hence, the free sites for CTX adsorption increase by increasing the adsorbent dosage from 0.5 to 2 g/L and consequently it causes the enhancement of the removal efficiency [44,45]. The resultant removal efficiency are in line with Mousavi and et al. who reported the removal efficiency range of 35 to 72% when applied the commercially activated carbon from Merck company in dosage range 0.4 to 1.6, respectively [46].

Table 6
Validation of optimized conditions for CTX adsorption on the PAC-MNPs.

pH	Time (min)	Concentration (mg/L)	Adsorbent dose (g/L)	Temperature (k)	Removal efficiency of ceftriaxone (%)	Desirability
3.14	90.00	10.00	1.99	298.00	97.18	0.972

3.5. The effect of temperature on CTX adsorption

The effect of temperature on the CTX removal efficiency were investigated in three temperature values of 298.15, 305.65 and 313.15 K. As Fig. 5 illustrates, the maximum adsorption of CTX was obtained at 298.15 K, and the removal efficiency of CTX decreases through increasing of temperature.

3.6. The effect of contact time on CTX adsorption

The contact time were surveyed to determine the optimum time with high CTX removal efficiency (Fig. 4). In the present research, the adsorption was increased as time proceeded and the maximum adsorption was found to be at 90 min. The increases in adsorption by passing time means the fact that more empty sites are available for adsorption, however, from time 90 min onwards, remaining empty sites were filled gradually by CTX and adsorption is difficult to occur due to less driving force between adsorbent and adsorbate [47]. Mousavi et al. reported that by increasing the time, the removal efficiency of Diazenon using chloride ammonium containing activated carbon increases, which is similar to the results of present work [48]. In a study conducted by Sari et al. on antimony removal by chitosan activated carbon, a contact time in range 5–90 min were considered, and reported that as time proceeds to 90 min, the removal efficiency increases and after that the efficiency was approximately constant [49].

3.7. Data analyzes

Nowadays, RSM is applied to analyze the multi-variable experiments and optimize the responses. As shown in Eq. (20), the empirical relationship between experimental variables and removal efficiency was determined using the RSM method;

$$\begin{aligned}\textbf{Ceftriaxone removal} = {} & +72.80-(6.00^{*}X_1)\\ & +(4.03^{*}X_2)-(3.67^{*}X_3)\\ & +(3.46^{*}X_4)-(4.00^{*}X_5)\\ & +(0.000^{*}X_1{}^{*}X_2)-(0.13^{*}X_1{}^{*}X_3)-(0.13^{*}X_1{}^{*}X_4)\\ & +(0.000^{*}X_1{}^{*}X_5)\\ & +(0.000^{*}X_2{}^{*}X_3)-(0.12^{*}X_2{}^{*}X_4)\\ & +(0.000^{*}X_2{}^{*}X_5)+(0.18^{*}X_3{}^{*}X_4)\\ & +(0.000^{*}X_3{}^{*}X_5)\\ & +(0.000^{*}X_4{}^{*}X_5)-\left(0.90^{*}X_1{}^{2}\right)\\ & +\left(1.15^{*}X_2{}^{2}\right)+\left(2.75^{*}X_3{}^{2}\right)\\ & +\left(0.63^{*}X_4{}^{2}\right)+\left(0.10^{*}X_5{}^{2}\right)\end{aligned} \quad (20)$$

As can be seen in equation expressed above, some factors or variables are positive sign, some negative effects. Negatively signed variables (X_1, X_3, and X_5) mean decreases in the removal efficiency by increasing in value. Positively signed variables (X_2 and X_4) have direct relation to removal efficiency achieved. Statistical parameters summarized in Table 5 reflect that the regression model with p-value = 0.0001 and F-Value = 1976.03 is statistically significant and is appropriate to spatial modeling. It should be noted that all parameters examined in the present work (p-value < 0.05) were significant in confidence interval 95%. This suggests that the model is significant and can appropriately explain the relationship between response and independent variables [50]. As presented in Table 5. The values of determination coefficient (R^2), adjusted-R^2 and Predicted-R^2 were 95.73%, 99.89%, and 99.80%. Fig. 6 shows the predicted values versus the experimental values for removal efficiency. It means that there is a good agreement between Predicted-R^2 and Adjusted -R^2 [51]. The "Adequate Precision" ratio of the model was found to be 159.444. Ratios >4 indicate that there is an adequate signal for the model [14].

Table 7
Isotherm and kinetic coefficients obtained from isotherm models.

Isotherm models			Kinetic models		
Model	Parameter	Value	Model	Parameter	Value
Langmuir	q_{max} (mg/g)	28.93	Pseudo-first order	q_e (mg/g)	6.46
	K_l (L/mg)	0.259		K_l (min^{-1})	0.004
	R^2	0.9961		R^2	0.9226
Freundlich	n	2.43	Pseudo-second	q_e (mg/g)	25.12
	K_f	6.59	order	K_2(g mg^{-1} min^{-1})	0.028
	R^2	0.964		R^2	0.9998
Temkin	q_m	5.39	Intra-particle	Kp	0.32
	K_t	3.67	diffusion	K_i (mg g^{-1} $min^{-0.5}$)	−21.62
	R^2	0.9673		R^2	0. 0.9685

3.8. Optimization using the desirability function

Design Expert 10.0 was applied to determine the optimum conditions for optimal removal efficiency. For this aim, the maximum CTX removal efficiency was defined as response and influencing parameters were considered in their range. Table 6 shows the numerically optimal value of each affecting parameter in CTX removal efficiency. According to results obtained from BBD, the maximum removal efficiency under optimum conditions i.e. contact time = 90.00 min, pH = 3.14, CTX initial concentration = 10.00 mg/L, adsorbent dosage = 1.99 g/L and temperature = 298.00 K was occurred to be 97.18%. The CTX removal efficiency in real conditions was evaluated to be 94.35. As presented in Table 6, the removal efficiency for response variable in BBD model and laboratory conditions are in strong agreement, which emphasize validity and precision of model. The findings indicated that RSM is useful and suitable tool for optimization CTX removal using PAC-MNPs.

3.9. Isotherms of CTX adsorption

The values of parameters associated with equilibrium isotherms of CTX removal onto synthesized PAC-MNPs are shown on Table 7. As can be concluded from the obtained results and what are observed in Table 7, the correlation coefficient of Langmuir is greater than those in Freundlich and Temkin model. As such, correlation coefficients in Langmuir, Freundlich and Temkin models are in respect R^2 = 0.9961, R^2 = 0.964 and R^2 = 0.9673. therefore, it can be reported that adsorption process is fitted to Langmuir isotherm. According to Table 6, the high value of R^2 obtained from the Langmuir model shows that the CTX adsorption on the PAC- MNPs probably follows the monolayer mechanism and the surface of the produced adsorbent is homogeneous [30]. The separation factor (R_L) value was between 0 and 1, indicating a favorable adsorption of CTX molecules onto PAC- MNPs. Liu et al. reported the optimum isotherm for Ceflaxine removal with activated carbon, by contrast, Liu et al. reported Langmuir isotherm as optimum isotherm for Noroflaxine using activated carbon [39,52].

3.10. Kinetics of CTX adsorption

The equations derived by Pseudo-first-order, Pseudo-second-order and Intra-particle diffusion kinetic models for adsorption of CTX onto

Table 8
The values of thermodynamic parameters for the adsorption of CTX on the PAC.

Temperature(°K)	lnkc	ΔG° (kJ/mol)	ΔH° (kJ/mol)	ΔS° (kJ/mol.K)
293	2.12	5.181		
308	2.08	5.330	−40.96	0.0081
323	2.07	5.57		

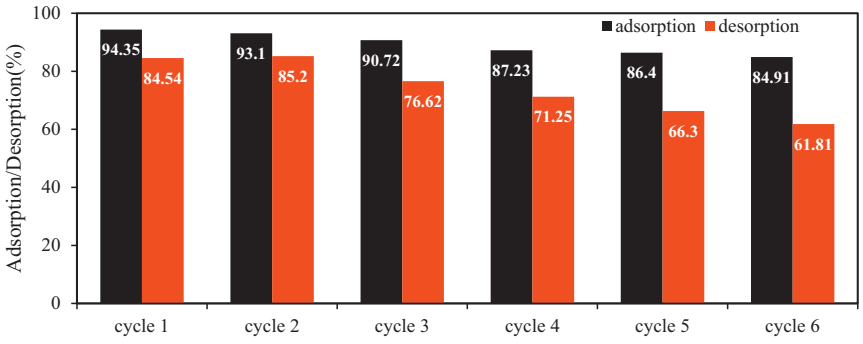

Fig. 7. CTX adsorption on the PAC-MNPs adsorbent under six adsorption–desorption cycles.

PAC-MNPs are presented in Table 7. The regression coefficient (R^2) and compatibility between q_e (experiment) with q_e (calculate) used to choose the best kinetic models. The results showed the pseudo-second-order model with $R^2 > 0.9998$ can be better described adsorption of CTX, that exhibits the rate-limiting is chemisorption and sharing of electrons from sorbent and adsorbate involving covalent forces [53]. In addition $q_{e,cal}$ at the pseudo-second–order compared to other models were more closer with $q_{e,exp}$. The similar studies confirm these results and are line with this research [39,52].

3.11. Thermodynamics of CTX adsorption

The calculated constants of thermodynamic model for the CTX adsorption on the PAC-MNPs is presented in Table 8. As the obtained results in Table 8 shows, the both values of ΔG° and ΔH° are negative. By contrast, the value of ΔS° obtained positive. A negative value ΔG° in our studies exhibits that the process of CTX removal with PAC-MNPs is spontaneous. The value of ΔH° is negative that confirms the adsorption process is exothermic in nature. Decreasing of ΔG° with increasing temperature indicates that the adsorption process at higher temperature is undesirable. The ΔS° value is positive, and increasing the randomness at the solid/solution interface during the CTX adsorption could be expected; besides, the positive ΔS° value corresponds to a rise in the freedom degree of the adsorbed species.

Xu et al. studied the Performance of rattle-type magnetic mesoporous silica spheres in the adsorption of single and binary antibiotics and concluded that rising the solution temperature decreases the adsorption capacity of antibiotics Tetracyclin and Solfametazin [54].

3.12. Reusability of PAC-MPNs

Adsorption-desorption of CTX by PAC-MPNs were performed in batch condition and shown in Fig. 7. Mentioned figure shows that reusability of PAC-MPNs slightly reduced after the six successive sorption–desorption cycles. Therefore, it can be suggested that PAC-MPNs can be repeatedly used for CTX sorption without many losses in initial sorption efficiency. Furthermore, >61.81% adsorbed CTX could be desorbed/recovered in the presence of methanol in the sixth cycle which can be used in different cases like industrial applications.

4. Conclusion

The magnetic nanoparticles of PAC-Fe_3O_4 with combining iron oxide nanoparticles and powder activated carbon were successfully synthesized and used in the removal of CTX from aqueous environments. The Box–Behnken design (BBD) was found to be a valuable tool to find optimal conditions for the procedure through a response surface study. The magnetic activated carbon with a high removal efficiency and perfect magnetic separation performance was examined by considering influencing parameters including the initial concentration, contact time, temperature, adsorbent dosage and pH. The present study demonstrated that the CTX removal using MNPs-PAC increases as both the adsorbent dosage and contact time increase, and it decreases when the pH, initial concentration of CTX and the temperature are increased. The optimum conditions for the present research were determined, including pH = 3.14, contact time = 90 min, temperature = 298 K, and adsorbent dosage = 1.99 g/L. Equilibrium and kinetic studies indicated that the adsorption was fitted with Langmuir and pseudo-second-order, respectively, Thermodynamic studies also showed that the CTX adsorption on PAC-MPNs has been spontaneous and exothermic. The results of this study indicated that PAC-MPNs could be satisfactorily used for removing CTX from aqueous environments due to high adsorption and easy and quick separation.

Conflict of interest

Author declares there is no conflict of interest regarding this publication.

Acknowledgement

The authors would like to gratefully appreciate Iran University of Medical Sciences for financial supports (Grant No. 94-05-27-27467).

References

[1] X. Guo, D. Li, J. Wan, X. Yu, Preparation and electrochemical property of TiO 2/nano-graphite composite anode for electro-catalytic degradation of ceftriaxone sodium, Electrochim. Acta 180 (2015) 957–964.
[2] S. Nasseri, A.H. Mahvi, M. Seyedsalehi, K. Yaghmaeian, R. Nabizadeh, M. Alimohammadi, G.H. Safari, Degradation kinetics of tetracycline in aqueous solutions using peroxydisulfate activated by ultrasound irradiation: effect of radical scavenger and water matrix, J. Mol. Liq. 241 (2017) 704–714.
[3] M. Farzadkia, A. Esrafili, M.A. Baghapour, Y.D. Shahamat, N. Okhovat, Degradation of metronidazole in aqueous solution by nano-ZnO/UV photocatalytic process, Desalin. Water Treat. 52 (2014) 4947–4952.
[4] V.M. Mboula, V. Hequet, Y. Gru, R. Colin, Y. Andres, Assessment of the efficiency of photocatalysis on tetracycline biodegradation, J. Hazard. Mater. 209 (2012) 355–364.
[5] M. Kermani, F. Bahrami Asl, M. Farzadkia, A. Esrafili, S. Salahshour Arian, M. Khazaei, Y. Dadban Shahamat, D. Zeynalzadeh, Heterogeneous catalytic ozonation by Nano-MgO is better than sole ozonation for metronidazole degradation, toxicity reduction, and biodegradability improvement, Desalin. Water Treat. 57 (2016) 16435–16444.
[6] X. Guo, J. Wan, X. Yu, Y. Lin, Study on preparation of SnO 2-TiO 2/Nano-graphite composite anode and electro-catalytic degradation of ceftriaxone sodium, Chemosphere 164 (2016) 421–429.
[7] E. Reynoso, M.B. Spesia, N.A. García, M.A. Biasutti, S. Criado, Riboflavin-sensitized photooxidation of ceftriaxone and cefotaxime. Kinetic study and effect on Staphylococcus aureus, J. Photochem. Photobiol. B Biol. 142 (2015) 35–42.
[8] M.H.S. Teixeira, L. Vilas-Boas, V. Gil, F. Teixeira, Complexes of ciprofloxacin with metal ions contained in antacid drugs, J. Chemother. 7 (1995) 126–132.
[9] J. Chen, Y.-S. Liu, J.-N. Zhang, Y.-Q. Yang, L.-X. Hu, Y.-Y. Yang, J.-L. Zhao, F.-R. Chen, G.-G. Ying, Removal of antibiotics from piggery wastewater by biological aerated filter system: treatment efficiency and biodegradation kinetics, Bioresour. Technol. 238 (2017) 70–77.
[10] A.C. Reina, A.B. Martínez-Piernas, Y. Bertakis, C. Brebou, N.P. Xekoukoulotakis, A. Agüera, J.A.S. Pérez, Photochemical degradation of the carbapenem antibiotics imipenem and meropenem in aqueous solutions under solar radiation, Water Res. 128 (2018) 61–70.

[11] R. Rostamian, H. Behnejad, A comprehensive adsorption study and modeling of antibiotics as a pharmaceutical waste by graphene oxide nanosheets, Ecotoxicol. Environ. Saf. 147 (2018) 117–123.
[12] H. Pasalari, H.R. Ghaffari, A.H. Mahvi, M. Pourshabanian, A. Azari, Activated carbon derived from date stone as natural adsorbent for phenol removal from aqueous solution, Desalin. Water Treat. 72 (2017) 406–417.
[13] F. An, X. Feng, B. Gao, Adsorption of aniline from aqueous solution using novel adsorbent PAM/SiO2, Chem. Eng. J. 151 (2009) 183–187.
[14] A.J. Jafari, B. Kakavandi, R.R. Kalantary, H. Gharibi, A. Asadi, A. Azari, A.A. Babaei, A. Takdastan, Application of mesoporous magnetic carbon composite for reactive dyes removal: process optimization using response surface methodology, Korean J. Chem. Eng. 33 (2016) 2878–2890.
[15] A. Azari, M. Gholami, Z. Torkshavand, A. Yari, E. Ahmadi, B. Kakavandi, Evaluation of basic violet 16 adsorption from aqueous solution by magnetic zero valent iron-activated carbon nanocomposite using response surface method: isotherm and kinetic studies, J. Mazandaran Univ. Med. Sci. 24 (2015) 333–347.
[16] M. Yegane badi, A. Azari, A. Esrafili, E. Ahmadi, M. Gholami, Performance evaluation of magnetized multiwall carbon nanotubes by Iron oxide nanoparticles in removing fluoride from aqueous solution, J. Mazandaran Univ. Med. Sci. 25 (2015) 128–142.
[17] S.T. Danalıoğlu, Ş.S. Bayazit, Ö.K. Kuyumcu, M.A. Salam, Efficient removal of antibiotics by a novel magnetic adsorbent: magnetic activated carbon/chitosan (MACC) nanocomposite, J. Mol. Liq. 240 (2017) 589–596.
[18] X. Zhang, W. Guo, H.H. Ngo, H. Wen, N. Li, W. Wu, Performance evaluation of powdered activated carbon for removing 28 types of antibiotics from water, J. Environ. Manag. 172 (2016) 193–200.
[19] B. Kakavandi, A. Esrafili, A. Mohseni-Bandpi, A.J. Jafari, R.R. Kalantary, Magnetic Fe3O4@ C nanoparticles as adsorbents for removal of amoxicillin from aqueous solution, Water Sci. Technol. 69 (2014) 147–155.
[20] D. Krishna, K.S. Krishna, R.P. Sree, Response surface modeling and optimization of chromium (vi) removal from aqueous solution using borasus flabellifer coir powder, Int. J. Appl. Sci. Eng. 11 (2013) 213–226.
[21] L.-n. Shi, Y.-M. Lin, X. Zhang, Z.-l. Chen, Synthesis, characterization and kinetics of bentonite supported nZVI for the removal of Cr (VI) from aqueous solution, Chem. Eng. J. 171 (2011) 612–617.
[22] N. Yang, S. Zhu, D. Zhang, S. Xu, Synthesis and properties of magnetic Fe 3 O 4-activated carbon nanocomposite particles for dye removal, Mater. Lett. 62 (2008) 645–647.
[23] R. RezaeiKalantary, A. JonidiJafari, B. Kakavandi, S. Nasseri, A. Ameri, A. Azari, Adsorption and magnetic separation of lead from synthetic wastewater using carbon/Iron oxide nanoparticles composite, J. Mazandaran Univ. Med. Sci. 24 (2014) 172–183.
[24] A. Bandhu, S. Mukherjee, S. Acharya, S. Modak, S. Brahma, D. Das, P. Chakrabarti, Dynamic magnetic behaviour and Mössbauer effect measurements of magnetite nanoparticles prepared by a new technique in the co-precipitation method, Solid State Commun. 149 (2009) 1790–1794.
[25] R. Valenzuela, M.C. Fuentes, C. Parra, J. Baeza, N. Duran, S. Sharma, M. Knobel, J. Freer, Influence of stirring velocity on the synthesis of magnetite nanoparticles (Fe3O4) by the co-precipitation method, J. Alloys Compd. 488 (2009) 227–231.
[26] G. Gnanaprakash, J. Philip, T. Jayakumar, B. Raj, Effect of digestion time and alkali addition rate on physical properties of magnetite nanoparticles, J. Phys. Chem. B 111 (2007) 7978–7986.
[27] G. Gnanaprakash, S. Mahadevan, T. Jayakumar, P. Kalyanasundaram, J. Philip, B. Raj, Effect of initial pH and temperature of iron salt solutions on formation of magnetite nanoparticles, Mater. Chem. Phys. 103 (2007) 168–175.
[28] F. Vereda, J. de Vicente, R. Hidalgo-Álvarez, Influence of a magnetic field on the formation of magnetite particles via two precipitation methods, Langmuir 23 (2007) 3581–3589.
[29] R.A. Latour, The Langmuir isotherm: a commonly applied but misleading approach for the analysis of protein adsorption behavior, J. Biomed. Mater. Res. Part A 103 (2015) 949–958.
[30] B. Djahed, E. Shahsavani, F. Khalili Naji, A.H. Mahvi, A novel and inexpensive method for producing activated carbon from waste polyethylene terephthalate bottles and using it to remove methylene blue dye from aqueous solution, Desalin. Water Treat. 57 (2016) 9871–9880.
[31] S.G. Wang, Y. Ma, Y.J. Shi, W.X. Gong, Defluoridation performance and mechanism of nano-scale aluminum oxide hydroxide in aqueous solution, J. Chem. Technol. Biotechnol. 84 (2009) 1043–1050.
[32] K.V. Kumar, Linear and non-linear regression analysis for the sorption kinetics of methylene blue onto activated carbon, J. Hazard. Mater. 137 (2006) 1538–1544.
[33] A. Esrafili, R. Rezaei Kalantary, A. Azari, E. Ahmadi, M. Gholami, Removal of diethyl phthalate from aqueous solution using persulfate-based (UV/Na2S2O8/Fe2+) advanced oxidation process, J. Mazandaran Univ. Med. Sci. 25 (2016) 122–135.
[34] E. Çalışkan, S. Göktürk, Adsorption characteristics of sulfamethoxazole and metronidazole on activated carbon, Sep. Sci. Technol. 45 (2010) 244–255.
[35] J. Rivera-Utrilla, G. Prados-Joya, M. Sánchez-Polo, M. Ferro-García, I. Bautista-Toledo, Removal of nitroimidazole antibiotics from aqueous solution by adsorption/bioadsorption on activated carbon, J. Hazard. Mater. 170 (2009) 298–305.
[36] E.C. Salihi, Adsorption of Metamizole sodium by activated carbon in simulated gastric and intestinal fluids, J. Turk. Chem. Soc. Section A Chem. 5 (2017) 237–246.
[37] N.N. Nassar, Rapid removal and recovery of Pb (II) from wastewater by magnetic nanoadsorbents, J. Hazard. Mater. 184 (2010) 538–546.
[38] O. Gutierrez-Muñiz, G. García-Rosales, E. Ordoñez-Regil, M. Olguin, A. Cabral-Prieto, Synthesis, characterization and adsorptive properties of carbon with iron nanoparticles and iron carbide for the removal of As (V) from water, J. Environ. Manag. 114 (2013) 1–7.
[39] W. Liu, J. Zhang, C. Zhang, L. Ren, Sorption of norfloxacin by lotus stalk-based activated carbon and iron-doped activated alumina: mechanisms, isotherms and kinetics, Chem. Eng. J. 171 (2011) 431–438.
[40] B. Kakavandi, R. Rezaei Kalantary, A. Jonidi Jafari, A. Esrafily, A. Gholizadeh, A. Azari, Efficiency of powder activated carbon magnetized by Fe3O4 nanoparticles for amoxicillin removal from aqueous solutions: equilibrium and kinetic studies of adsorption process, Iran. J. Health Environ. 7 (2014) 21–34.
[41] M. Shokri, G. Isapour, S. Shamsvand, B. Kavousi, Photocatalytic Degradation of Ceftriaxone in Aqueous Solutions by Immobilized TiO2 and ZnO Nanoparticles: Investigating Operational Parameters.
[42] V. Meshko, L. Markovska, M. Mincheva, A. Rodrigues, Adsorption of basic dyes on granular activated carbon and natural zeolite, Water Res. 35 (2001) 3357–3366.
[43] R.I. Yousef, B. El-Eswed, H. Ala'a, Adsorption characteristics of natural zeolites as solid adsorbents for phenol removal from aqueous solutions: kinetics, mechanism, and thermodynamics studies, Chem. Eng. J. 171 (2011) 1143–1149.
[44] A. Afkhami, M. Saber-Tehrani, H. Bagheri, Modified maghemite nanoparticles as an efficient adsorbent for removing some cationic dyes from aqueous solution, Desalination 263 (2010) 240–248.
[45] I.D. Mall, V.C. Srivastava, N.K. Agarwal, I.M. Mishra, Removal of Congo red from aqueous solution by bagasse fly ash and activated carbon: kinetic study and equilibrium isotherm analyses, Chemosphere 61 (2005) 492–501.
[46] A. Alahabadi, G. Moussavi, K. Yaghmaeian, H. Karemisany, Adsorption Potential of the Granular Activated Carbon for the Removal of Amoxicillin from Water, 2014.
[47] C.-H. Wu, Adsorption of reactive dye onto carbon nanotubes: equilibrium, kinetics and thermodynamics, J. Hazard. Mater. 144 (2007) 93–100.
[48] G. Moussavi, H. Hosseini, A. Alahabadi, The investigation of diazinon pesticide removal from contaminated water by adsorption onto NH 4 Cl-induced activated carbon, Chem. Eng. J. 214 (2013) 172–179.
[49] A. Sari, M. Tuzen, İ. Kocal, Application of chitosan-modified pumice for antimony adsorption from aqueous solution, Environ. Prog. Sustain. Energy 00 (2017) 1587–1596.
[50] A. Azari, B. Kakavandi, R.R. Kalantary, E. Ahmadi, M. Gholami, Z. Torkshavand, M. Azizi, Rapid and efficient magnetically removal of heavy metals by magnetite-activated carbon composite: a statistical design approach, J. Porous. Mater. 22 (2015) 1083–1096.
[51] B. Kakavandi, M. Jahangiri-rad, M. Rafiee, A.R. Esfahani, A.A. Babaei, Development of response surface methodology for optimization of phenol and p-chlorophenol adsorption on magnetic recoverable carbon, Microporous Mesoporous Mater. 231 (2016) 192–206.
[52] H. Liu, W. Liu, J. Zhang, C. Zhang, L. Ren, Y. Li, Removal of cephalexin from aqueous solutions by original and Cu (II)/Fe (III) impregnated activated carbons developed from lotus stalks kinetics and equilibrium studies, J. Hazard. Mater. 185 (2011) 1528–1535.
[53] S. Swain, T. Patnaik, P. Patnaik, U. Jha, R. Dey, Development of new alginate entrapped Fe (III)–Zr (IV) binary mixed oxide for removal of fluoride from water bodies, Chem. Eng. J. 215 (2013) 763–771.
[54] L. Xu, J. Dai, J. Pan, X. Li, P. Huo, Y. Yan, X. Zou, R. Zhang, Performance of rattle-type magnetic mesoporous silica spheres in the adsorption of single and binary antibiotics, Chem. Eng. J. 174 (2011) 221–230.